Spatial solitons and stability in the one-dimensional and the two-dimensional generalized nonlinear Schrödinger equation with fourth-order diffraction and parity-time-symmetric potentials

C. G. L. Tiofack,[1,3] F. II Ndzana,[1,2,3] A. Mohamadou,[2,3,4,5] and T. C. Kofane[1,3,5]

[1]*Laboratory of Mechanics, Department of Physics, Faculty of Science, University of Yaounde I, P.O. Box 812, Yaounde, Cameroon*

[2]*Condensed Matter Laboratory, Department of Physics, Faculty of Science, University of Maroua, P.O. Box 814, Maroua, Cameroon*

[3]*Centre d'Excellence Africain des Technologies de l'Information et de la Communication (CETIC), University of Yaounde I, P.O. Box 812, Yaounde, Cameroon*

[4]*Abdus Salam International Centre for Theoretical Physics, P.O. Box 538, Strada costiera 11, I-34014, Trieste, Italy*

[5]*Max Planck Institute for the Physics of Complex Systems, Nothnitzer Strasse 38, 01187, Dresden, Germany*

(Received 28 December 2017; published 9 March 2018)

We investigate the existence and stability of solitons in parity-time ($\mathcal{PT}$)-symmetric optical media characterized by a generic complex hyperbolic refractive index distribution and fourth-order diffraction (FOD). For the linear case, we demonstrate numerically that the FOD parameter can alter the $\mathcal{PT}$-breaking points. For nonlinear cases, the exact analytical expressions of the localized modes are obtained both in one- and two-dimensional nonlinear Schrödinger equations with self-focusing and self-defocusing Kerr nonlinearity. The effect of FOD on the stability structure of these localized modes is discussed with the help of linear stability analysis followed by the direct numerical simulation of the governing equation. Examples of stable and unstable solutions are given. The transverse power flow density associated with these localized modes is also discussed. It is found that the relative strength of the FOD coefficient can utterly change the direction of the power flow, which may be used to control the energy exchange among gain or loss regions.

DOI: 10.1103/PhysRevE.97.032204

I. INTRODUCTION

Over the past decade, and since they were originally proposed by Bender and coworkers [1,2], systems characterized by parity-time ($\mathcal{PT}$)-symmetric Hamiltonians have become a subject of intense research efforts. The interest in these systems arises from their fundamental property to exhibit real spectra, while non-Hermitian, thus providing an intriguing alternative to standard Hermitian quantum mechanics. Bender *et al.* also found that, for a $\mathcal{PT}$-symmetric Hamiltonian, there exists a critical threshold above which its eigenvalues are not real but become complex, and the system undergoes a phase transition because of the spontaneous $\mathcal{PT}$-symmetry breaking [1]. Transition through this exceptional point is the most typical scenario of $\mathcal{PT}$-symmetry breaking, which arises in a more general context of non-Hermitian physics [3].

Due to an analogy between the Schrödinger equation in quantum mechanics and the equation for slowly varying mode amplitude in optics, $\mathcal{PT}$-symmetric phenomena can be observed in nonconservative optical systems with mutually balanced gain and loss [4–6]. To achieve the balance between gain and loss, the refractive index of the system should satisfy the relation $n(x) = n^*(-x)$, which means that the real and imaginary parts of the complex refractive index distribution should be even and odd functions of position, respectively [6]. As shown in several studies, $\mathcal{PT}$-symmetric optical arrangements can exhibit several interesting and counterintuitive properties, which are otherwise unattainable in standard configurations [7–10]. These include, for example, non-Hermitian Bloch oscillations [11], abrupt phase transitions [12], nonreciprocity [8,9], unidirectional invisibility [13], loss-induced super scattering and gain-induced absorption [14], and mode selection in $\mathcal{PT}$-symmetric lasers [15], as well as existence of coherent lasing absorbing modes [16]. Finally $\mathcal{PT}$-symmetric concepts have also been used in plasmonics [17], optical metamaterials [18], and coherent atomic medium [19]. These findings, in turn, have stimulated considerable research activity in the nonlinear $\mathcal{PT}$-symmetric systems as well.

In the last few years, various $\mathcal{PT}$-symmetric potentials have been introduced to the nonlinear Schrödinger (NLS) equations, which have been shown to possess stable and unstable solitons of different types [5,20–25]. Particulary, the existence of different nonlinear localized modes has been studied analytically as well as numerically in the NLS equation with complex $\mathcal{PT}$-symmetric Scarf-II potential [5,20,21,26], periodic potential [5,20], Gaussian potential [27], Bessel potential [28], Rosen-Morse Potential [29], and harmonic potential [24]. In addition to these, nonlinear modes have been studied for other complex $\mathcal{PT}$-symmetric potentials bearing nonlinear optical systems such as competing nonlinearity [30], saturable nonlinearity [31], and logarithmically saturable nonlinearity [32].

It is particularly noteworthy that many of the above mentioned $\mathcal{PT}$-symmetric potentials have concentrated on models of NLS equation with a second order diffraction or dispersion term. However, in the study of ultra-short optical pulse propagation, the higher-order diffraction or dispersion effects cannot be neglected [33,34]. Specifically, fourth-order dispersion has been demonstrated to play an important role in fiber optics [35,36]. Additionally, modulational instability in NLS-type models with high-order dispersion have been extensively investigated [37–40]. In a recent study, the existence and stability of gap solitons in the semi-infinite gap of a $\mathcal{PT}$-symmetric

optical lattice with a higher-order diffraction were examined [41,42]. It was found that the Bloch bands and band gaps of $\mathcal{PT}$-symmetric optical lattice depend crucially on the coupling constant of the fourth-order diffraction (FOD). In these works, the localized solutions are obtained with the help of some numerical techniques. In fact, very few models of $\mathcal{PT}$-symmetric potential with higher-order diffraction or dispersion possess exact analytical expressions for the localized modes. More recently, under $\mathcal{PT}$-symmetric potentials, different kinds of exact bright solitons and their fascinating properties were discussed in the third-order NLS equation [43]. Thus far, nobody has investigated exact solitons solutions in $\mathcal{PT}$-symmetric structures with higher-order diffraction or dispersion.

Our aim in this paper is to study analytically and numerically the linear and nonlinear modes of the FOD NLS equation with a generic complex hyperbolic $\mathcal{PT}$-symmetric potential. The exact expressions of such solutions are obtained in both one-dimensional (1D) and two-dimensional (2D) NLS equations. These solitons are shown to be stable through the linear-stability analysis and by means of direct simulations, in wide ranges of the governing parameters.

This paper is organized as follows. In Sec. II we introduce the 1D NLS equation with FOD in the presence of complex hyperbolic $\mathcal{PT}$-symmetric potentials. The exact expression of a localized solution of this model is obtained for both self-focusing and self-defocusing nonlinear cases. We investigate the effect of the FOD coefficient on the spectra of linear problem and stability of nonlinear mode. We show that some of these solutions can be stable, which is confirmed by both the linear stability analysis and numerical time evolutions of the complex NLS equation. Section III deals with the analytical localized modes and their linear stability in two dimensions. Finally, in Sec. IV the main results of the paper are briefly summarized.

II. LOCALIZED MODES IN $\mathcal{PT}$-SYMMETRIC COMPLEX POTENTIAL WITH FOURTH-ORDER DIFFRACTION

A. Model equation

We consider optical wave propagation in a Kerr nonlinear $\mathcal{PT}$-symmetric potential with an FOD coefficient. In this case, evolution of the dimensionless light field envelope $\psi(z,x)$ is governed by the 1D NLS equation [41,42]:

$$i\frac{\partial\psi}{\partial z}+\frac{\partial^2\psi}{\partial x^2}-\beta\frac{\partial^4\psi}{\partial x^4}+[V(x)+iW(x)]\psi+g|\psi|^2\psi=0, \tag{1}$$

where z is the propagation distance, x is the transverse coordinate, β is the coupling constant of the FOD, and $g=\pm1$ represent the self-focusing and self-defocusing nonlinearity, respectively. $V(x)$ and $W(x)$ are the real and imaginary parts of the complex $\mathcal{PT}$-symmetric potential such that $V(-x)=V(x)$ and $W(-x)=-W(x)$. Physically, $V(x)$ is responsible for the bending and slowing of light, and $W(x)$ can lead to either amplification (gain) or absorption (loss) of light within an optical material. In the absence of gain-and-loss distribution $W(x)$, band gaps and lattice solitons were investigated in Eq. (1) with a periodic potential and FOD coefficient [44].

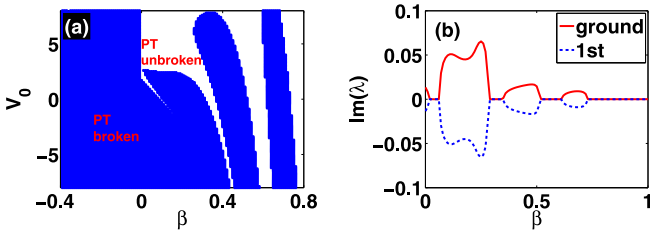

FIG. 1. (a) The unbroken or broken $\mathcal{PT}$-symmetric phase produced by linear eigenvalue problem (4) with $\mathcal{PT}$-symmetric potential (3). (b) Imaginary part of the eingavalue λ as a function of the FOD coefficient β at $V_0=1$. The parameter $W_0=2$.

We focus on the stationary solutions of Eq. (1) in the form $\psi(z,x)=\phi(x)e^{i\nu z}$, where ν is the real propagation constant and the complex function $\phi(x)$ satisfies the stationary NLS equation:

$$\frac{d^2\phi(x)}{dx^2}-\beta\frac{d^4\phi(x)}{dx^4}+[V(x)+iW(x)]\phi(x)+g|\phi|^2=\nu\phi(x), \tag{2}$$

which can be solved by using numerical methods. To study analytically the localized soliton solution of Eq. (2), we consider the following $\mathcal{PT}$-symmetric potential:

$$\begin{aligned}V(x)&=V_0\mathrm{sech}^2(x)+V_1\mathrm{sech}^4(x),\\ W(x)&=\mathrm{sech}(x)\tanh(x)[W_0+W_1\mathrm{sech}^2(x)],\end{aligned} \tag{3}$$

with $V_1=\beta(\mu^4+35\mu^2+24)$, $W_1=10\mu\beta(\mu^2+5)$, and $\mu=W_0(1-5\beta)/3$. The constants V_0, V_1, W_0, and W_1 represent the depths of the real and imaginary parts of the potential. The $\mathcal{PT}$-symmetric potential (3) is a hyperbolic version of the quantum-mechanical potential introduced by Scarf [45]. These two functions are bounded and $V(x)$, $W(x)\to0$ as $|x|\to\infty$. Moreover, the gain-and-loss distribution can be always balanced in Eq. (1) since $\int_{-\infty}^{+\infty}W(x)\,dx=0$.

B. $\mathcal{PT}$ linear mode with fourth-order diffraction

In the absence of the nonlinearity ($g=0$), Eq. (2) becomes the following eigenvalue problem:

$$L\Phi(x)=\lambda\Phi(x),\quad L=\partial_x^2-\beta\partial_x^4+V(x)+iW(x), \tag{4}$$

with λ and $\Phi(x)$ being the eigenvalue and the localized eigenfunction, respectively. For the case $\beta=0$, Eq. (3) reduces to the standard Scarff-II potential in which the Hamiltonian of (4) exhibits an entirely real spectrum ($\mathcal{PT}$ unbroken phase) provided that $|W_0|<V_0+1/4$ [46]. For the general case with $\beta\neq0$, and by using numerical calculation, Fig. 1(a) exhibits the broken or unbroken $\mathcal{PT}$-symmetric phases on the (V_0,β) space. It is seen that, for fixed V_0, there always exists a critical value of β beyond which the symmetry-breaking phase transition makes the spectra complex-valued. For a given value $W_0=2$, it can also be seen that for $\beta<0$, the broken region is predominantly obtained. On the other hand, for $\beta>0$, the unbroken region appears and exhibits a complicated structure. For the given parameters $V_0=1$ and $W_0=2$, and varying the FOD coefficient β, the spontaneous symmetry breaking occurs from two lowest states at seven points about β [see Fig. 1(b)].

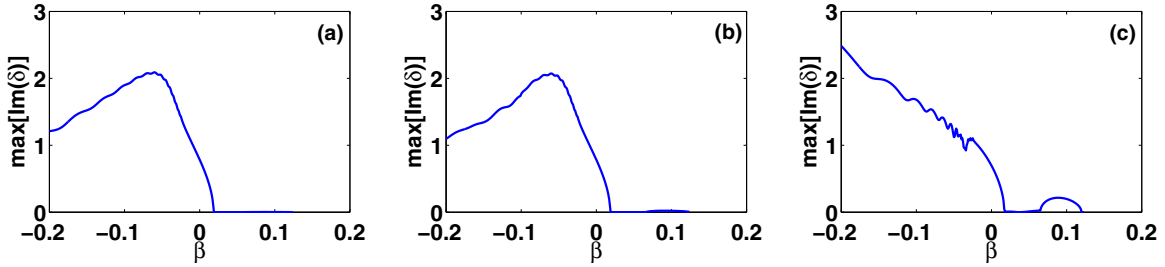

FIG. 2. The perturbation growth rate of solitons versus β with different values of W_0: (a) $W_0 = 0.01$, (b) $W_0 = 0.1$, (c) $W_0 = 1$ in the focusing nonlinearity $g = 1$. In all cases we have considered $V_0 = -0.5$.

C. $\mathcal{PT}$ nonlinear mode and stability

The exact bright soliton of Eq. (2) with $\mathcal{PT}$-symmetric potential (3) for both self-focusing and self-defocusing cases can be found in the form

$$\phi(x) = \phi_0 \mathrm{sech}(x) \exp\{i\mu \arctan[\sinh(x)]\}. \tag{5}$$

Here the propagation constant ν, the phase number μ, and the soliton amplitude ϕ_0 are related to the potential parameters and the FOD coefficient through

$$\nu = 1 - \beta, \quad \mu = \frac{W_0}{3}(1 - 5\beta),$$
$$\phi_0 = \sqrt{\frac{2 - V_0 + \mu^2 - 5\beta(4 + 5\mu^2)}{g}}, \tag{6}$$

where $g[2 - V_0 + \mu^2 - 5\beta(4 + 5\mu^2)] > 0$ is the existence condition of the solution.

From Eq. (6), we can find that the FOD coefficient influences the different parameters of the solution. In the particular case where $\beta = 0$, the solution (5) reduces to the known ones as given in Ref. [5].

For the nonlinear modes given in Eq. (5), the Poynting vector $S = \frac{i}{2}(\phi\phi_x^* - \phi^*\phi_x) = \mu\phi_0^2 \mathrm{sech}^3(x)$. For $\beta = 0$, S is everywhere positive if $W_0 > 0$ [5,25]. In presence of the FOD coefficient $\beta \neq 0$, the sign of S is not always positive or negative definite and is dependent on both parameters W_0 and β. From the expression of μ obtained in (6), it is clearly seen that S remains positive if $W_0 > 0$ and $\beta < 1/5$. This suggests in this case that the power flow in the $\mathcal{PT}$ cell is in one direction, i.e., from the gain towards loss domain. The total power of the stationary localized solution is $P = \int_{-\infty}^{\infty} |\phi(x,z)|^2 \, dx = 2\phi_0^2$, which is independent on the the propagation distance z and thus conserved.

In order to investigate the effect of the FOD parameter on the linear stability properties of the self-trapped nonlinear modes obtained here, we consider small perturbation to the solution $\psi(x,z)$, in the form [23,24,30]

$$\psi(x,z) = \{\phi(x) + \epsilon[F(x)e^{i\delta z} + G^*(x)e^{-i\delta^* z}]\}e^{i\nu z}, \tag{7}$$

where $\epsilon \ll 1$, $F(x)$ and $G(x)$ are the perturbation eigenfunctions of the linearized eigenvalue problem, and δ measures the growth rate of the perturbation instability. Substituting Eq. (7) into Eq. (1) and linearizing with respect to ϵ, we obtain the following linear eigenvalue problem:

$$\begin{bmatrix} \hat{L} & g\phi^2(x) \\ -g\phi^{*2}(x) & -\hat{L}^* \end{bmatrix} \begin{bmatrix} F(x) \\ G(x) \end{bmatrix} = \delta \begin{bmatrix} F(x) \\ G(x) \end{bmatrix}, \tag{8}$$

where $\hat{L} = -\mu + \partial_{xx} - \beta\partial_{xxxx} + V(x) + iW(x) + 2g|\phi|^2$. The eigenvalue problem (8) can be solved numerically with the help of Fourier collocation method [47]. The stability of the perturbed soliton $\psi(x,z)$ is related to the imaginary parts $\mathrm{Im}(\delta)$ of all eigenvalues δ. If $|\mathrm{Im}(\delta)| > 0$, then the solution $\psi(x,z)$ will grow exponentially with z (i.e., it is unstable), otherwise the solution $\psi(x,z)$ is stable. In the existence range of the numerically found solitons, the dependence of the the perturbation growth rate (the most unstable growth rate) on the FOD coefficient is exhibited in Figs. 2 and 3. It is clearly shown that for a fixed value of V_0, the stable regions shrink with the increase of W_0 value, in the case of both focusing [Figs. 2(a)–2(c)] and defocusing nonlinearities [Figs. 3(a)–3(c)]. By comparing these two figures, we observe that the defocusing nonlinearities enjoy a wider range of stable solitons than the focusing cases.

For the attractive case $g = 1$, the numerically computed linear stability spectra are plotted in Fig. 4(b1) for stable modes and in Fig. 4(b2) for unstable ones (for different parameters V_0, W_0, and β). The stable mode leads to a double-well potential

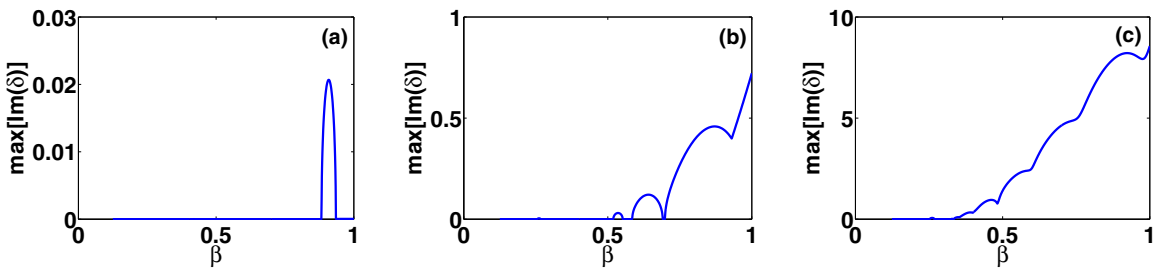

FIG. 3. The perturbation growth rate of solitons versus β with different values of W_0: (a) $W_0 = 0.01$, (b) $W_0 = 0.1$, (c) $W_0 = 1$ in the defocusing nonlinearity $g = -1$. In all cases we have considered $V_0 = -0.5$.

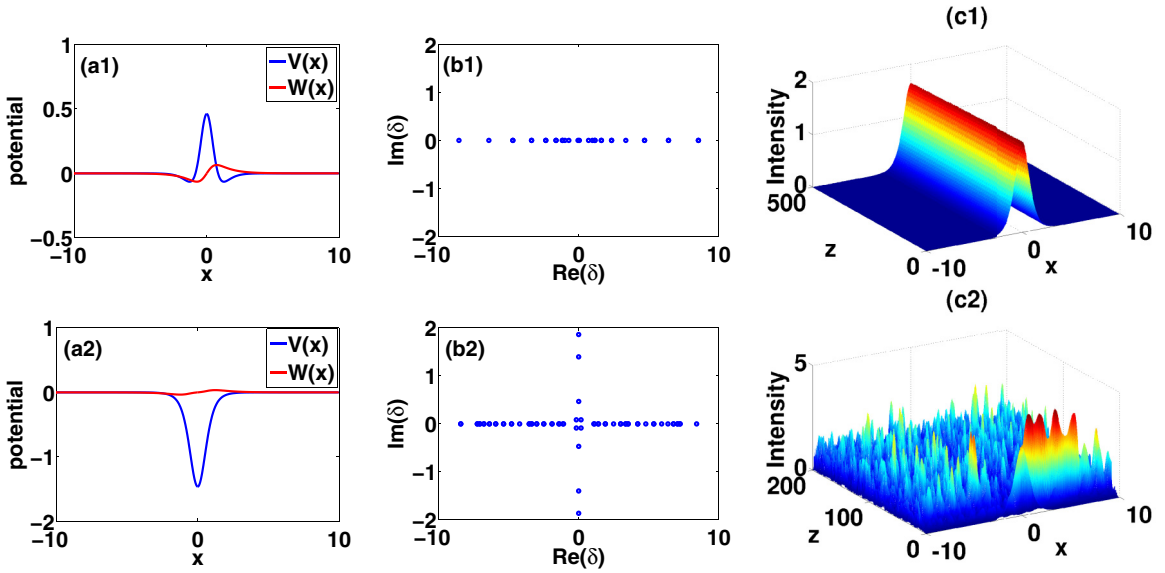

FIG. 4. (a1, a2) Real and imaginary parts of $\mathcal{PT}$-symmetric potentials given in Eq. (3). (b1, b2) Numerically computed linear stability spectra in the case of self-focusing nonlinearity $g = 1$. (c1) Stable and (c2) unstable propagations of nonlinear modes described in Eq. (2). (a1, b1, c1) $V_0 = -0.5$, $W_0 = 0.1$, $\beta = 0.04$. (a2, b2, c2) $V_0 = -0.5$, $W_0 = 0.1$, $\beta = -0.04$.

[see Fig. 4(a1)], while the unstable one leads to a single-well potential [see Fig. 4(a2)]. To validate the linear stability results, we have simulated the propagation of exact soliton (5) under an initial random noise perturbation up to 1% of its amplitude for different parameters. Corresponding stable and unstable propagations, in agreement with the linear stability analysis, are displayed in Figs. 4(c1) and 4(c2), respectively.

For the repulsive case $g = -1$, the results of linear stability spectra are displayed in Fig. 5(b1) for stable modes and in Fig. 5(b2) for unstable ones. The two cases lead to only a barrier potential [see Figs. 5(a1) and 5(a2)]. Further, we have also tested the propagation dynamics of the exact nonlinear modes (5) under an initial random noise perturbation up to 1% of its amplitude. Typical simulation examples, shown in Figs. 5(c1) and 5(c2), are in good agreements with the prediction of linear stability analysis.

III. LOCALIZED MODES IN 2D $\mathcal{PT}$-SYMMETRIC COMPLEX POTENTIAL

We now consider the 2D NLS equation with a $\mathcal{PT}$-symmetric potential and a FOD coefficient [48]:

$$i\frac{\partial\psi}{\partial z} + \Delta\psi - \beta\Delta^2\psi + [V(x,y) + iW(x,y)]\psi + g|\psi|^2\psi = 0, \quad (9)$$

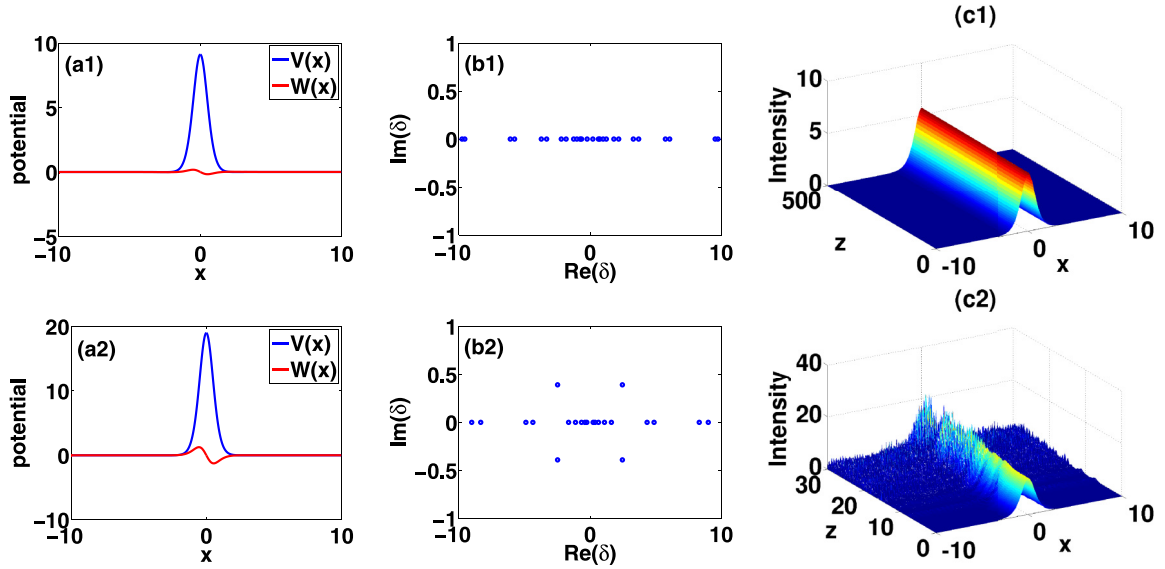

FIG. 5. (a1, a2) Real and imaginary parts of $\mathcal{PT}$-symmetric potentials given in Eq. (3). (b1, b2) Numerically computed linear stability spectra in the case of self-defocusing nonlinearity $g = -1$. (c1) Stable and (c2) unstable propagations of nonlinear modes described in Eq. (2). (a1, b1, c1) $V_0 = -0.5$, $W_0 = 0.1$, $\beta = 0.4$. (a2, b2, c2) $V_0 = -0.5$, $W_0 = 0.1$, $\beta = 0.8$.

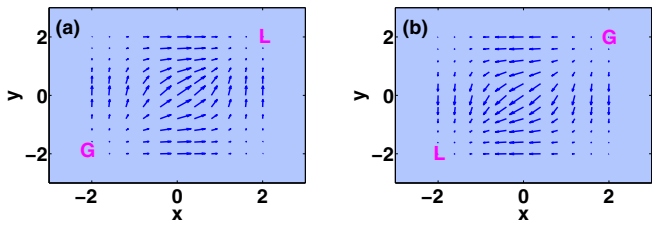

FIG. 6. Transverse power flow vector indicating the power flow (a) from gain towards loss regions when $\beta = 0.1$; (b) from loss towards gain regions when $\beta = 0.25$. The other parameters are $V_0 = -4$, $W_0 = 1$, $g = 1$.

where $\psi = \psi(x,y,z)$ is a complex field envelope function, Δ is the 2D Laplacian in the (x,y) plane, and Δ^2 is the so-called bi-Laplacian. The 2D complex potentials, which obey the $\mathcal{PT}$-symmetric requirements $V(-x,-y) = V(x,y)$ and $W(-x,-y) = -W(x,y)$, are considered as

$$V(x,y) = V_{01} \sum_{\sigma=x,y} \mathrm{sech}^2(\sigma) + V_1 \sum_{\sigma=x,y} \mathrm{sech}^4(\sigma) - V_{02} \prod_{\sigma=x,y} \mathrm{sech}^2(\sigma),$$

$$W(x,y) = W_{01} \sum_{\sigma=x,y} \mathrm{sech}(\sigma)\tanh(\sigma) + W_1 \sum_{\sigma=x,y} \mathrm{sech}^3(\sigma)\tanh(\sigma), \quad (10)$$

where the constants V_1 and W_1 are given by Eq. (6), $V_{01} = 2 + \mu^2 - 5\beta(4 + 5\mu^2)$, $V_{02} = 2 - V_0 + a^2 - 5\beta(4 + 5a^2)$, and $W_{01} = W_0[1 + 5\beta(5\beta - 2)]$.

We find the exact analytical solutions of Eq. (9) with the FOD coefficient β and $\mathcal{PT}$-symmetric potential (10) in the form

$$\psi(x,y,z) = \phi(x,y)\exp[i\nu z + i\theta(x,y)], \quad (11)$$

where $\nu = 2(1-\beta)$, the phase $\theta(x,y)$, and soliton $\phi(x,y)$ are obtained as

$$\phi(x,y) = \phi_0 \mathrm{sech}(x)\mathrm{sech}(y),$$
$$\theta(x,y) = \mu\{\tan^{-1}[\sinh(x)] + \tan^{-1}[\sinh(y)]\}. \quad (12)$$

The soliton amplitude ϕ_0 and the phase number μ are given by Eq. (6).

The transverse power flow density for these 2D solutions is calculated as

$$\vec{S}(x,y) = \mu\phi_0^2[\mathrm{sech}^3(x), \mathrm{sech}^3(y)], \quad (13)$$

whose positive or negative sign depends on the sign of the phase number μ. Then if $W_0 = 0$, or $\beta = 1/5$, we have $\mu = 0$ and the power does not flow. If $W_0 > 0$, $\beta < 1/5$, we have $\mu > 0$ and the power flows from gain towards loss [see Fig. 6(a)]. In other cases, $\mu < 0$ and the power flows from loss toward gain [see Fig. 6(b)]. The above results indicate that the relative strength of the FOD coefficient and the sign of gain-loss distribution can utterly change the direction of the power flow, which may be used to control the energy exchange among gain or loss regions. In addition, the conserved power related to the solution (12) is given by $P = 4\phi_0^2$, which is conserved.

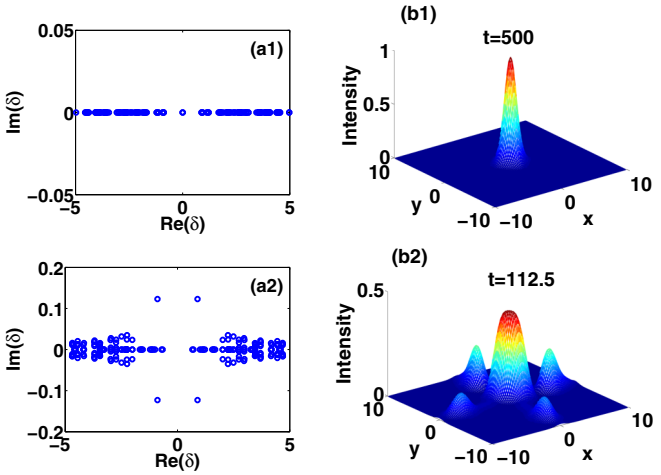

FIG. 7. (a1, a2) Plots of the linear stability eigenvalue spectra of the 2D solitons in the case of self-focusing nonlinearity $g = 1$. (b1) and (b2) plots of the corresponding stable and unstable intensity evolution. The parameters are (a1, b1) $V_0 = -2$, $W_0 = 0.1$, $\beta = 0.15$; (a2, b2) $V_0 = -1$, $W_0 = 1$, $\beta = 0.03$.

The linear stability of the 2D localized modes, obtained here, is studied by considering the 2D generalization of the eigenvalue problem given in (8). In Figs. 7(a1)–7(a2) and Figs. 8(a1)–8(a2), we have shown the numerically computed eigenvalue spectra for the focusing and defocusing nonlinearity, respectively. To obtain the corresponding intensity evolution, we have performed the direct numerical simulation of Eq. (9) by taking the initial profile as $\psi(x,y,0) = \phi(x,y)e^{i\theta(x,y)}$. The results are shown in Figs. 7(b1) and 8(b1) for stable propagation, and in Figs. 7(b2) and 8(b2) for unstable propagation. The results of numerical simulations are in good

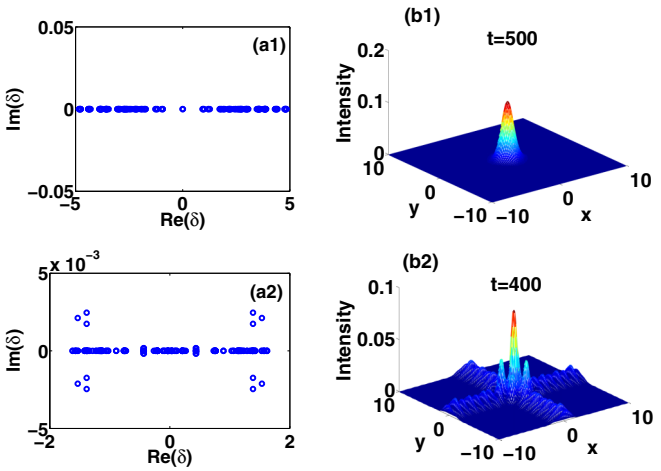

FIG. 8. (a1, a2) Plots of the linear stability eigenvalue spectra of the 2D solitons in the case of self-defocusing nonlinearity $g = -1$. (b1, b2) Plots of the corresponding stable and unstable intensity evolution. The parameters are (a1, b1) $V_0 = 0.1$, $W_0 = 0.5$, $\beta = 0.1$; (a2, b2) $V_0 = 5$, $W_0 = 0.1$, $\beta = -0.14$.

agreement with the predictions produced above by the linear stability analysis.

IV. CONCLUSION

In this work, we have investigated analytically and numerically the existence and properties of new classes of 1D and 2D spatial solitons supported by a complex hyperbolic $\mathcal{PT}$-symmetric potential in the presence of fourth-order diffraction and Kerr nonlinearity. For the linear version of the model, it is shown numerically that the $\mathcal{PT}$-symmetric phases may admit several breaking points due to the presence of the fourth-order diffraction parameter. Then, in the presence of the Kerr nonlinearity, the closed form expressions for the localized modes in such 1D and 2D self-focusing and self-defocusing Kerr nonlinear media are obtained. A linear stability analysis corroborated by the direct numerical simulations reveals that these analytical localized modes can propagate while being stable for certain values of the fourth-order diffraction coefficient. The transverse power flow associated with these complex solitons has also been computed. Our results suggest new possibilities for experimental and theoretical studies about the dynamics of nonlinear waves in more complex $\mathcal{PT}$-symmetric potentials and higher-order diffraction.

ACKNOWLEDGMENTS

C.G.L.T. acknowledges the support of the Laboratoire d'Excellence CEMPI: Centre Européen pour les Mathématiques, la Physique et leurs Interactions.

[1] C. M. Bender and S. Boettcher, Phys. Rev. Lett. **80**, 5243 (1998).
[2] C. M. Bender, D. C. Brody, and H. F. Jones, Phys. Rev. Lett. **89**, 270401 (2002).
[3] I. Rotter, Phys. Rev. E **65**, 026217 (2002).
[4] R. El-Ganainy, K. G. Makris, D. N. Christodoulides, and Z. H. Musslimani, Opt. Lett. **32**, 2632 (2007).
[5] Z. H. Musslimani, K. G. Makris, R. El-Ganainy, and D. N. Christodoulides, Phys. Rev. Lett. **100**, 030402 (2008).
[6] K. G. Makris, R. El-Ganainy, D. N. Christodoulides, and Z. H. Musslimani, Phys. Rev. Lett. **100**, 103904 (2008).
[7] C. E. Rüter, K. G. Makris, R. El-Ganainy, D. N. Christodoulides, M. Segev, and D. Kip, Nat. Phys **6**, 192 (2010).
[8] K. G. Makris, R. El-Ganainy, D. N. Christodoulides, and Z. H. Musslimani, Phys. Rev. A **81**, 063807 (2010).
[9] B. Midya, B. Roy, and R. Roychoudhury, Phys. Lett. A **374**, 2605 (2010).
[10] S. V. Suchkov, F. Fotsa-Ngaffo, A. Kenfack-Jiotsa, A. D. Tikeng, T. C. Kofane, Y. S. Kivshar, and A. A. Sukhorukov, New J. Phys. **18**, 065005 (2016).
[11] S. Longhi, Phys. Rev. A **82**, 031801 (2010).
[12] A. Guo, G. J. Salamo, D. Duchesne, R. Morandotti, M. Volatier-Ravat, V. Aimez, G. A. Siviloglou, and D. N. Christodoulides, Phys. Rev. Lett. **103**, 093902 (2009).
[13] Z. Lin, H. Ramezani, T. Eichelkraut, T. Kottos, H. Cao, and D. N. Christodoulides, Phys. Rev. Lett. **106**, 213901 (2011).
[14] S. M. Feng, Opt. Express **24**, 1291 (2016).
[15] M. A. Miri, P. Likamwa, and D. N. Christodoulides, Opt. Lett. **37**, 764 (2012).
[16] L. Feng, Z. J. Wong, R. M. Ma, Y. Wang, and X. Zhang, Science **346**, 972 (2014).
[17] H. Benisty, A. Degiron, A. Lupu, A. De Lustrac, S. Chenais, S. Forget, M. Besbes, G. Barbillon, A. Bruyant, S. Blaize, and G. Lerondel, Opt. Express **19**, 18004 (2011).
[18] G. Castaldi, S. Savoia, V. Galdi, A. Alù, and N. Engheta, Phys. Rev. Lett. **110**, 173901 (2013).
[19] J. Sheng, M. A. Miri, D. N. Christodoulides, and M. Xiao, Phys. Rev. A **88**, 041803(R) (2013).
[20] Z. H. Musslimani, K. G. Makris, R. El-Ganainy, and D. N. Christodoulides, J. Phys. A **41**, 244019 (2008).
[21] Z. Shi, X. Jiang, X. Zhu, and H. Li, Phys. Rev. A **84**, 053855 (2011).
[22] F. K. Abdullaev, Y. V. Kartashov, V. V. Konotop, and D. A. Zezyulin, Phys. Rev. A **83**, 041805(R) (2011).
[23] S. Nixon, L. Ge, and J. Yang, Phys. Rev. A **85**, 023822 (2012).
[24] D. A. Zezyulin and V. V. Konotop, Phys. Rev. A **85**, 043840 (2012).
[25] Z. Yan, Y. Chen, and Z. Wen, Chaos **26**, 083109 (2016); Y. Chen, Z. Yan, D. Mihalache, and B. A. Malomed, Sci. Rep. **7**, 1257 (2017).
[26] Z. Yan, Z. Wen, and C. Hang, Phys. Rev. E **92**, 022913 (2015).
[27] S. Hu, X. Ma, and W. Hu, Phys. Rev. A **84**, 043818 (2011).
[28] S. Hu and W. Hu, J. Phys. B: At. Mol. Opt. Phys. **45**, 225401 (2012).
[29] B. Midya and R. Roychoudhury, Phys. Rev. A **87**, 045803 (2013).
[30] A. Khare, S. M. Al-Marzoug, and H. Bahlouli, Phys. Lett. A **376**, 2880 (2012).
[31] W.-P. Hong and Y. D. Jung, Phys. Lett. A **379**, 676 (2015).
[32] K. Zhan, H. Tian, X. Li, X. Xu, Z. Jiao, and Y. Jia, Sci. Rep. **6**, 32990 (2016).
[33] W.-J. Liu, B. Tian, H.-Q. Zhang, T. Xu, and H. Li, Phys. Rev. A **79**, 063810 (2009).
[34] S. Roy, S. K. Bhadra, and G. P. Agrawal, Phys. Rev. A **79**, 023824 (2009).
[35] M. Tlidi and L. Gelens, Opt. Lett. **35**, 306 (2010).
[36] G. Kozyreff, M. Tlidi, A. Mussot, E. Louvergneaux, M. Taki, and A. G. Vladimirov, Phys. Rev. Lett. **102**, 043905 (2009).
[37] F. Kh. Abdullaev, S. A. Darmanyan, S. Bischoff, P. L. Christiansen, and M. P. Sorensen, Opt. Commun. **108**, 60 (1994).
[38] S. Pitois and G. Millot, Opt. Commun. **226**, 415 (2003).
[39] M. Droques, A. Kudlinski, G. Bouwmans, G. Martinelli, A. Mussot, A. Armaroli, and F. Biancalana, Opt. Lett. **38**, 3464 (2013).
[40] A. Mohamadou, C. G. L. Tiofack, T. B. Ekogo, J. Atangana, T. C. Kofane, and K. Porsezian, J. Mod. Opt. **58**, 924 (2011).
[41] L. Ge, M. Shen, C. Ma, T. Zang, and L. Dai, Opt. Express **22**, 29435 (2014).
[42] X. Zhu, Z. Shi, and H. Li, Opt. Commun. **382**, 455 (2017).
[43] Y. Chen and Z. Yan, Sci. Rep. **6**, 23478 (2016).
[44] J. T. Cole and Z. H. Musslimani, Phys. Rev. A **90**, 013815 (2014).
[45] F. L. Scarf, Phys. Rev. **112**, 1137 (1958).
[46] M. Znojil, J. Phys. A **33**, L61 (2000); Z. Ahmed, Phys. Lett. A **282**, 343 (2001).
[47] J. Yang, J. Comp. Phys. **227**, 6862 (2008).
[48] J. T. Cole and Z. H. Musslimani, Physica D **313**, 26 (2015).